Hβ Line Widths as an Orientation Indicator for Low-Ionization Broad Absorption Line Quasars

Brian Punsly[1]

and

Shaohua Zhang[2]

ABSTRACT

There is evidence from radio-loud quasars to suggest that the distribution of the Hβ broad emission line (BEL) gas is arranged in a predominantly planar orientation, and this result may well also apply to radio-quiet quasars. This would imply that the observed full width at half maximum (FWHM) of the Hβ BELs is dependent on the orientation of the line of sight to the gas. If this view is correct then we propose that the FWHM can be used as a surrogate, in large samples, to determine the line of sight to the Hβ BELs in broad absorption line quasars (BALQSOs). The existence of broad UV absorption lines (BALs) means that the line of sight to BALQSOs must also pass through the BAL out-flowing gas. It is determined that there is a statistically significant excess of narrow line profiles in the SDSS DR7 archival spectra of low ionization broad absorption line quasars (LoBALQSOs), indicating that BAL gas flowing close to the equatorial plane does not commonly occur in these sources. We also find that the data is not well represented by random lines of sight to the BAL gas. Our best fit indicates two classes of LoBALQSOs, the majority ($\approx 2/3$) are polar outflows, that are responsible for the enhanced frequency of narrow line profiles, and the remainder are equatorial outflows. We further motivated the line of sight explanation of the narrow line excess in LoBALQSOs by considering the notion that the skewed distribution of line profiles is driven by an elevated Eddington ratio in BALQSOs. We constructed a variety of control samples comprised of nonLoBALQSOs matched to a de-reddened LoBALQSO sample in redshift, luminosity, black hole mass and Eddington ratio. It is demonstrated that the excess of narrow profiles

[1]4014 Emerald Street No.116, Torrance CA, USA 90503 and ICRANet, Piazza della Repubblica 10 Pescara 65100, Italy, brian.punsly@verizon.net or brian.punsly@comdev-usa.com

[2]Key Laboratory for Research in Galaxies and Cosmology, University of Sciences and Technology of China, China Academy of Science, Hefei, Anhui, 230026 China

persists within the LoBALQSO sample relative to each of the control samples with no reduction of the statistical significance. Thus, we eliminate the possibility that the excess narrow lines seen in the LoBALQSOs arise from an enhanced Eddington ratio.

Subject headings: (galaxies:) quasars: absorption lines — galaxies: jets — (galaxies:) quasars: general — accretion, accretion disks — black hole physics

1. Introduction

About 15% - 20% of quasars show broad UV absorption lines (originally defined as absorbing gas that is blue shifted at least 5,000 km/s relative to the QSO rest frame and displaying a spread in velocity of at least 2,000 km/s) (Weymann 1997; Hewett and Foltz 2003; Reichard et al. 2003; Trump et al 2006; Gibson et al 2009). Although evolutionary processes might be related to BAL outflows this does not seem to be the primary determinant. There is no indication that there is an excessive amount of radiation associated with reprocessed emission from dust as would be expected if the BALQSOs were in an evolutionary stage characterized by a large volume of dusty gas enshrouding the central AGN (Willott et al. 2003; Gallagher et al 2007). Also, the overall optical/UV spectra are strikingly similar to non-BALQSOs (Weymann et al. 1991; Reichard et al. 2003). Thus, it is widely believed that all or most radio quiet quasars have BAL flows, but the designation of a quasar as a BALQSO depends on whether the line of sight intersects the solid angle subtended by the outflow. This prevailing view is our fundamental assumption that motivates our search for a diagnostic that determines these preferred lines of sight. This is our primary working hypothesis and we explore possible effects that would be expected by preferred lines of sight.

The "standard model of quasars" is one of a hot accretion flow onto a black hole and a surrounding torus of molecular gas (Antonucci 1993). Theoretical treatments indicate that the BAL outflow can be an equatorial wind driven from the outer regions of a luminous accretion disk that is viewed at low latitudes, Murray et al (1995), or a bipolar flow launched from the inner regions of the accretion flow (Punsly 1999a,b). Furthermore, Elvis (2000), proposed a purely phenomenological model in which the BAL wind begins near or at the accretion disk and flows at mid-range latitudes arranged so as to propagate just above the surface of the distant dusty torus. It has also been proposed that there is more than one wind source (polar and equatorial) for the BAL winds that coexist in QSOs (Punsly 1999b; Proga and Kallman 2004). It has been further argued by Brotherton et al (2006) that observations rule out one preferred narrow range of lines of sight to the BAL wind. The

question is left open as to the distribution of lines of sights to BALQSOs, a question we hope to answer for LoBALQSOs in this study.

There is very little direct evidence that we have on the line of sight to the BAL region. The most direct method implemented so far is to use radio variability information (Zhou et al 2006; Ghosh and Punsly 2007). This information can be used to bound the size of the radio emitting gas then deduce that the radio emission must be viewed close to the polar axis and emanate from a relativistic jet, thereby avoiding the well known inverse Compton catastrophe (Marscher et al 1979; Kellermann & Pauliny-Toth 1969; Lind and Blandford 1985). However, this method will only find sources with a polar orientation and it is limited to a subset of those sources that have sufficient radio flux to make the measurement and multiple epochs of observation with compatible sensitivity, a very small subsample. Thus, another orientation indicator is needed in this field of research. In radio loud quasars, the dominance of the radio core relative to the large scale radio lobes is the standard orientation indicator (Wills and Browne 1986). Core dominant objects are polar, lobe dominant objects are viewed at large angles from the jet axis. Almost all BALQSOs are unresolved with the VLA, Becker et al (2000), but the radio fluxes are small and there is not sufficient sensitivity (and in many cases insufficient resolution) to get a meaningful estimate of core dominance. Furthermore, the spectra of BALQSOs are often similar to a special class of radio source, Gigahertz peaked radio sources, for which this orientation indicator might not even be applicable (Montenegro-Montes et al 2008).

A breakthrough paper in the field of BEL orientation was Wills and Browne (1986) which showed that there was an anti-correlation between radio core dominance and the FWHM of Hβ in radio loud quasars that was explained by a broad line region (BLR) that was predominantly planar. The existence of a planar distribution of low ionization BEL gas seems to carry over to the radio quiet regime as well. It was noted in Antonucci et al (1989); Maiolino et al (2002) that a planar distribution resolves the paradox that quasar Lyα equivalent widths (and BEL equivalent widths in general) imply column densities that should show the Lyman continuum in absorption and with all profiles heavily damped. But, no quasar BEL cloud has ever been convincingly seen in absorption (Antonucci et al 1989). Since a large fraction of the solid angle around quasar must be covered with low-ionization BEL gas, yet no Lyman continuum absorption has ever been convincingly detected from the BEL clouds, it must be that quasars oriented favorably for BEL absorption are not seen as quasars. The only plausible way to do this is by placing the low ionization BEL clouds within the solid angle of the torus, so that these objects are not seen as quasars from our point of view. Furthermore, the large covering factor of the continuum by the equatorial planar BEL gas distribution creates an enormous volume of ionized BEL gas, sufficient to produce these large equivalent widths. Lines of sight far above the equatorial

plane (in the hole of the dusty torus, as expected for exposed quasar nuclei, Antonucci (1993)) penetrate the relatively thin column densities orthogonal to the plane of the gas distribution, revealing the continuum in emission, with insufficient column density to produce damped Lyman absorption edges. This resolves the paradox. In conclusion, the notion of a planar distribution of low ionization BEL gas appears to be applicable to all quasars and suggests that the main ideas of Wills and Browne (1986) are relevant to predominantly radio quiet samples as well. There is no evidence of a difference between radio quiet and radio loud AGN in this regard. There are some differences in the spectra of radio loud and radio quiet quasars that have been noted in the literature that are not entirely understood (see eg. Corbin and Francis (1994); Corbin and Boroson (1996)), but do not clearly have a bearing on this point

Thusly motivated, we compiled the FWHM of low redshift, $0.4 < z < 0.8$, LoBALQSOs in the SDSS DR7 archives to look for orientation information. This redshift range insures that both Mg II and Hβ emission lines are visible. High ionization, CIV, absorption will not appear in these spectra thus, our analysis is limited to LoBALQSOs. First we compare the quasars showing LoBALs with those that do not. Then we simulate the distribution of Hβ FWHM that would be expected for different lines of sight. This information is used to discuss the line of sight to the BLR of LoBALQSOs.

2. The Distribution of Hβ in SDSS DR7

In the DR7 release we found 102 LoBALQSOs (out of a sample of 10,069 quasars) in the redshift range, $0.4 < z < 0.8$. The LoBALQSO determination is based on spectra with S/N > 7, using the criteria of continuous absorption over a velocity interval greater than 1600 km/s for a depth of at least 10% as in Zhang et al (2010) which see for a detailed discussion of this criteria. The fitting of the Hβ profile also follows the DR5 analysis of Zhang et al (2010). The distributions of Hβ FWHM of LoBALQSOs and non-LoBALQSOs from DR7 in this redshift range are compared in Figure 1. Because the bin populations of the LoBALQSOs are small, error bars were added to the bin frequencies. The horizontal error bars represent the width of the bins in Figure 1. The vertical (bin population) error bars are difficult to assess for small bin sizes, we chose to represent these with binomial statistics. It is notable from Figure 1 that there is a difference in the partial distributions of FWHM between the two samples for values smaller than 6,500 km/sec (a subsample that represents $\approx 80\%$ of the sources for both the total sample and the LoBALQSOs, separately). The LoBALQSOs are skewed toward lower FWHM in the partial distribution. The difference between these partial distributions is significant in both a K-S test (a null probability of 0.0178) and a

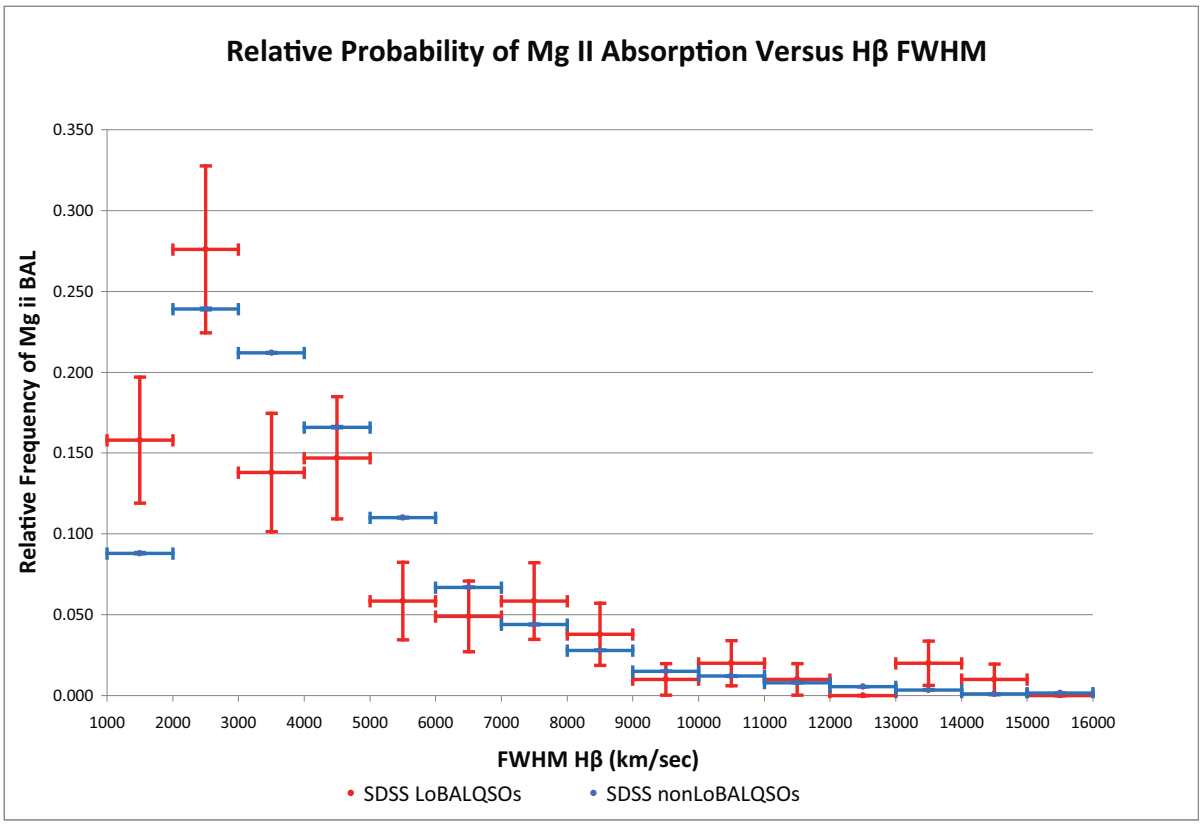

Fig. 1.— Comparison of the distributions of Hβ FWHM of LoBALQSOs and non-LoBALQSOs from DR7. Note the excess of narrow line profiles less than 2,500 km/s in the LoBALQSO population. The error bars are based on binomial statistics.

Wilcoxon Rank Sum Test (a null probability of 0.0028). Thus, formally, we conclude that the distribution of LoBALQSO FWHM is poorly described by the distribution of FWHM of non-BALQSOs. To understand more than this, we consider the effects of a preferred line of sight to the BAL region and an elevated Eddington ratio in LoBALQSOs.

3. Searching for an Alternative Physically Based Explanation

Before adopting a line of sight interpretation of the excess of narrow emission lines in the LoBALQSO population in Figure 1, we explore the possibility that the effect is driven by a physical difference in the black hole accretion system between the LoBALQSOs and other quasars. We explore three potential physical parameters: the bolometric luminosity, L_{bol}, the mass of the central black hole, M_{bh} and the Eddington ratio, $\Gamma = L_{bol}/L_{Edd}$. To do this, we create "matched subsamples" of the SDSS DR7 nonLoBALQSOs that are matched in optical luminosity, black hole mass and Eddington ratio to LoBALQSOs. It is demonstrated that the difference in FWHM between LoBALQSOs and nonLoBALQSOs that was noted in Figure 1 is just as pronounced in the "matched" nonLoBALQSO samples. Obviously, all the quasar properties can not be identical between two samples in all moments of the probability distributions. One must choose the most important parameter and optimize for that one. We pay particularly close attention to subsamples that are matched with respect to Γ.

In our opinion, $L_{optical} = \lambda L_{\lambda}(5100\mathring{A})$ is the most logical parameter to restrict if one is to construct matched subsamples for the following reasons:

1. $L_{optical}$ is directly measurable and the other quantities are derived in consort with many assumptions.

2. In Zhang et al (2010), Figure 6, it was shown that a comparison of 2MASS fluxes with SDSS fluxes that the rest frame near IR/optical colors are similarly distributed for LoBALQSOs and nonLoBALQSOs. Thus, this optically selected sample of LoBALQSO spectra show minimal reddening in the optical band, with a magnitude that is similar to that of the background galactic starlight contribution (Zhang et al 2010). We expect that $L_{optical}$ is representative of the intrinsic optical luminosity up to a small correction on the order of the galactic starlight. With these small de-reddening corrections, $L_{optical}$ is an acceptable surrogate for L_{bol} in either the LoBALQSO sample or nonLoBALQSO sample.[1]

[1]Note that if one were to cull the sample of LoBALQSOs from an IR flux limited sample, we would not

3. It is shown in Ganguly et al (2007) for HiBALQSOs and corroborated for LoBALQSOs in Figure 12 of Zhang et al (2010) that the biggest physical difference between BALQSOs and nonBALQSOs is that BALQSOs tend to have larger rest frame continuum fluxes.

The significant difference in the rest frame continuum flux noted in point 3 above, is driven largely by the lack of low values of $L_{optical}$ within the BALQSO population. This is expected by dynamical considerations, low values of radiation pressure do not produce enough force to drive outflows from the environs of a black hole (Murray et al 1995; Punsly 1999b). Figure 12 of Zhang et al (2010) indicates that there are very few DR5 LoBALQSOs with $L_{optical} < 4 \times 10^{44}$ ergs/sec. Thus, we construct matched samples by truncating the nonLoBALQSO DR7 sample on the low side. We create a variety of samples by varying the low end cutoff. We produced many such samples with a range of the derivable physical parameters designed to straddle those of the LoBALQSOs. Table 1 shows data for the various samples created with different cutoffs.

In Table 1, we list the physical parameters of various subsamples for the sake for comparison. Column 1 describes the types of sources, LoBALQSO or nonLoBALQSO, that comprise the sample. The second column gives the low end cutoff in $L_{optical}$ that was used to define the sample. The next column is the number of sources in the sample. The fourth column is the resultant average $L_{optical}$. The next two columns give the probability that the sources within the sample with FWHM < 6500 km/s are drawn from the same population as the LoBALQSOs with FWHM < 6500 km/s, for a Wilcoxon rank sum test and a K-S test. Columns 7 and 8 are the Eddington ratio and logarithm of the black hole mass, the derivation of which are given is the following paragraphs.

The sample called, "LoBALQSO de-reddened", is designed to compare the intrinsic luminosity of the LoBALQSOs to that of the nonLoBALQSOs. The reddening in the optical is small as noted above in point 2. Thus, our attempts to de-redden the sources are not likely to generate large errors, even if our assumptions are not highly accurate. Our main assumption is based on the DR5 composite spectra for LoBALQSOs and nonLoBALQSOs in Zhang et al (2010). In i-band, it was found that the LoBALQSO composite continuum had about 0.25 to 0.33 magnitudes of attenuation relative to the nonLoBALQSO composite continuum. The wavelength of interest in the rest frame, associated with $L_{optical}$, straddles

---

expect this to be true. The SDSS optical selection criteria will not find the more reddened LoBALQSOs that would be found in the IR samples. We also note that Zhang et al (2010) showed that the LoBALQSO spectra are significantly reddened in the ultraviolet and therefore $L_{UV} = \lambda L_{\lambda}(3000\mathring{A})$ is not a good surrogate for L_{bol}

Table 1: Physical Properties of Samples

Sample	cutoff 10^{44} [c]	Number	$L_{optical}$ 10^{45}[c]	P Wilcoxon	P K-S	Γ	Log(M_{bh}) $M_\odot$	OIII EW $\AA$
LBQSO[a]	0	102	1.05 ± 1.04	1	1	0.274 ± 0.247	8.51 ± 0.60	19.0 ± 29.4
LBQSO[a] (de-reddened)	0	102	1.32 ± 1.31	1	1	0.307 ± 0.276	8.56 ± 0.60	19.0 ± 29.4
NLBQSO[b]	0	10069	0.67 ± 0.75	0.0028	0.0178	0.214 ± 0.223	8.44 ± 0.46	26.7 ± 31.0
NLBQSO[b]	5	4824	1.03 ± 0.95	0.0008	0.0054	0.262 ± 0.261	8.57 ± 0.44	23.5 ± 21.3
NLBQSO[b]	6	3706	1.18 ± 1.04	0.0007	0.0051	0.277 ± 0.271	8.61 ± 0.44	23.2 ± 21.0
NLBQSO[b]	7	2919	1.32 ± 1.13	0.0005	0.0049	0.290 ± 0.282	8.64 ± 0.44	22.7 ± 20.4
NLBQSO[b]	8	2313	1.47 ± 1.22	0.0006	0.0061	0.304 ± 0.293	8.67 ± 0.44	22.3 ± 20.1
NLBQSO[b]	9	1860	1.62 ± 1.32	0.0005	0.0055	0.316 ± 0.300	8.70 ± 0.43	21.8 ± 19.6
NLBQSO[b]	10	1478	1.79 ± 1.43	0.0005	0.0078	0.332 ± 0.313	8.72 ± 0.43	21.4 ± 19.3
NLBQSO[b]	9[d]	1551	1.45 ± 0.87	0.0017	0.0152	0.321 ± 0.300	8.66 ± 0.42	16.3 ± 9.0
NLBQSO[b]	9[e]	1428	1.41 ± 0.68	0.0029	0.0258	0.326 ± 0.304	8.64 ± 0.42	15.2 ± 7.9

[a] ow ionization broad absorption line quasars

[b] Non-low ionization broad absorption line quasars

[c] ergs/s

[d] The O III line strength of the sample was cutoff from above to limit the sample to $< 10^{43}$ergs/s

[e] The O III line strength of the sample was cutoff from above to limit the sample to $< 8 \times 10^{42}$ergs/s

the high end of i-band and the low end of the less attenuated z-band. Thus, we expect that an average extinction of ≈ 0.25 magnitudes of attenuation in the rest frame at $5100\mathring{A}$ is a good approximation. The observed flux is the sum of the reddened AGN spectrum and the contribution of the host galactic starlight. Therefore, on average, we acknowledge that the rest frame $L_{opttical}$ computed from observed fluxes will be larger than it would have been if it were computed directly from the reddened continuum flux from the nucleus. The 0.25 magnitudes of attenuation is therefore a liberal upper limit to the average value of the attenuation and the intrinsic AGN continuum flux will tend to be over-predicted from the rest frame $L_{opttical}$ computed from observed fluxes. As such, our estimates will tend to be an upper limit to the intrinsic average $L_{opttical}$ of the LoBALQSOs. We used this number to de-redden $L_{optical}$: this amounts to multiplying each $L_{optical}$ in the LoBALQSO sample by 1.25 to get the intrinsic value of $L_{optical}$ in the de-reddened sample.

It is also of interest to compute the distributions of derived physical properties. First of all we estimate M_{bh} from the Hβ FWHM using the virial mass formula in equation (5) of Vestergaard and Peterson (2006),

$$M_{bh}(H\beta) = \\ 10^{6.91\pm0.02}\left[\left(\frac{F(H\beta)}{1000\mathrm{km/s}}\right)^2\left(\frac{\lambda L_\lambda(5100\mathring{A})}{10^{44}\mathrm{ergs/s}}\right)^{0.50}\right] . \quad (1)$$

The logarithm of the values are tabulated in the eighth column of Table 1. The de-reddened sample uses the de-reddened $L_{optical}$ in the formula.

The physical parameter of most relevance in certain previous studies is the Eddington ratio, Γ (Boroson 2002; Sulentic et al 2006). The interpretation of Boroson (2002) was largely driven by a principal component analysis of line properties. The BALQSOs tend to have weak, narrow Hβ emission lines, weak OIII lines and strong optical FeII lines, giving them low eigenvector 1 values. The claim is that a low value of eigenvector 1 is physical in origin and is driven by large a Eddington ratio (Boroson 2002). The corresponding explanation of the narrow Hβ excess that is seen in LoBALQSOs would be that these sources are very high Eddington ratio sources and this translates into a stronger ionizing flux which creates low ionization gas farther out in the gravitational potential (in units of gravitational radius), hence producing narrower Hβ.

The first step in the computation of Γ is to estimate L_{bol} from $L_{optical}$. Perhaps the most popular bolometric correction is that of Kaspi et al (2000), $L_{bol} = 9\lambda L_\lambda(5100)$. We note that this bolometric correction is predicated on $L_{optical}$ representing the intrinsic optical luminosity. This is not the case for the LoBALQSOs. Hence, the need for the de-reddened sample. The resultant Γ values are tabulated in the seventh column of Table 1. Since this

parameter has received much attention in the past, in the context of LoBALQSOs, we look at a particular matched subsample of nonLoBALQSOs in detail. The sample with a cutoff at 9×10^{44} ergs/sec is well matched to the de-redden distribution of Γ according to Table 1. We plot the distribution of Γ in Figure 2 for both the matched sample and the de-reddened sample. The distributions are indistinguishable in a statistical sense. The probability that the two samples are drawn from different distributions of Γ is only 0.249 according to a Wilcoxon rank sum test and 0.254 in a K-S test.

Next, we plot the distribution of Hβ FWHM for the matched sample and the LoBALQSOs (reddening does not affect the LoBALQSO FWHM distribution) in Figure 3. The distribution is very similar to Figure 1. We conclude that Γ is a negligible physical factor with regards to producing the excess of narrow Hβ profiles for LoBALQSOs in the Figure 1 and the LoBALQSOs in DR7 in general.

In terms of the eigenvector space, Boroson (2002) claimed that BALQSOs are associated with very small eigenvector 2 (large accretion rate) and extremely small eigenvector 1 (large Γ). Table 1, shows that the matched subsample in Figures 2 and 3 has a slightly higher average accretion rate (using the intrinsic $L_{optical}$ as a surrogate) and slightly higher Γ than the de-reddened LoBALQSOs. There are other samples in Table 1 that have slightly smaller values of $L_{optical}$ and/or Γ as well. For all these samples that surround the de-reddened LoBALQSOs in the 2-D parameter space, the excess of narrow lines in the de-reddened LoBALQSO sample persists with high statistical significance. Thus, there does not appear to be any physical properties associated with the location in the eigenvector parameter space that are responsible for the excess of narrow Hβ line widths in LoBALQSOs.

Finally, we explore the relationship to eigenvector 1 in more detail. In the last column of Table 1, we list the O III EW which has a large projection on eigenvector 1 (Boroson and Green 1992). Weak O III emission, in of itself, is not a plausible physical mechanism for launching a BALQSO wind, but it is possibly related to the BALQSO phenomenon on the basis of the previously quoted eigenvector space analysis (i.e., being very far from the accretion disk, the narrow line region is not a fundamental physical quantity that characterizes the black hole accretion system such as black hole mass, Eddington rate and bolometric luminosity). Exploring the luminosity of the O III emission can potentially provide insight into the interplay between eigenvector 1 and the existence of observed UV broad absorption lines. The LoBALQSOs in Table 1 have weak O III line strengths. None of the control samples that are created by means of a low end cutoff on $L_{optical}$ have an average O III EW as small the LoBALQSO sample. We would like the control smaples to straddle the average value of the OIII EW in the LoBALQSO sample in order to elucidate the connection between the Hβ FWHM and the O III EW. Thus, we constructed two modified

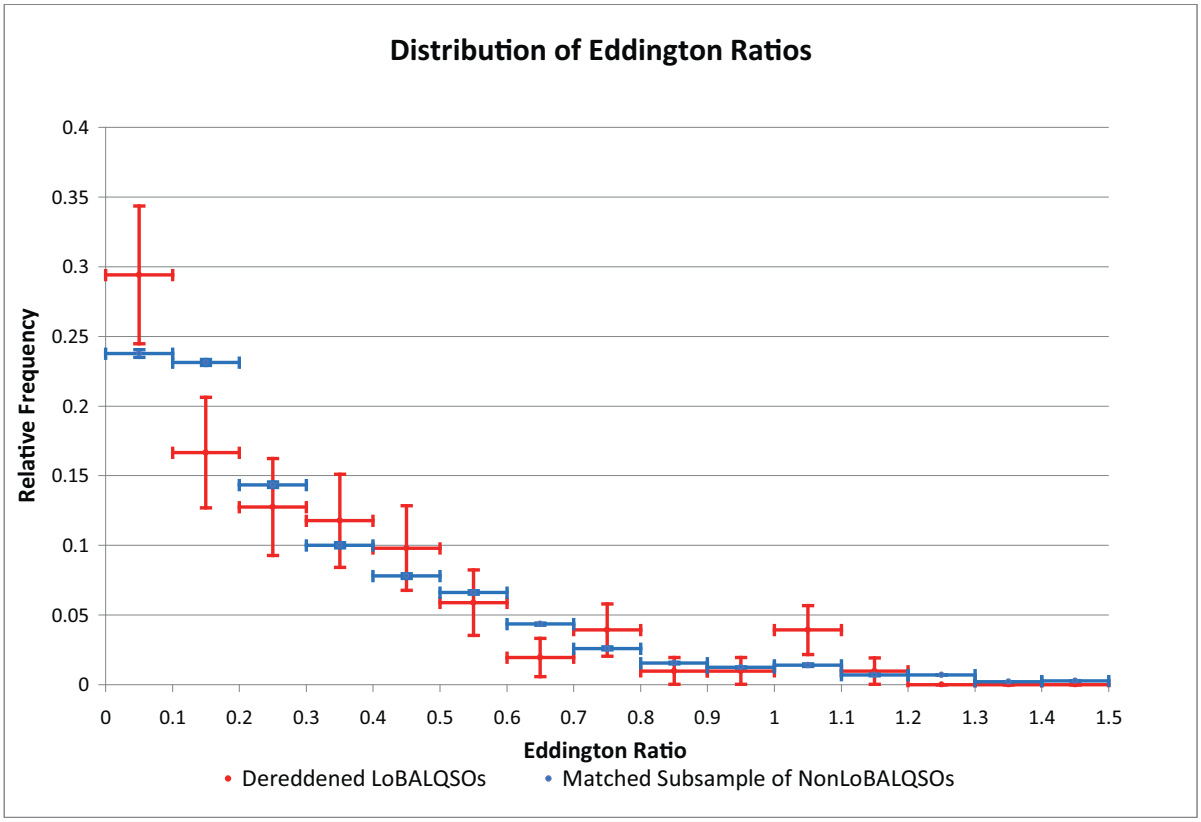

Fig. 2.— Comparison of the distributions of Γ for LoBALQSOs and the "matched" sample of non-LoBALQSOs from DR7. The matched sub-sample is created from the full SDSS nonLoBALQSOS sample by the condition $L_{optical} > 9 \times 10^{44}$ ergs/s. The error bars are based on binomial statistics.

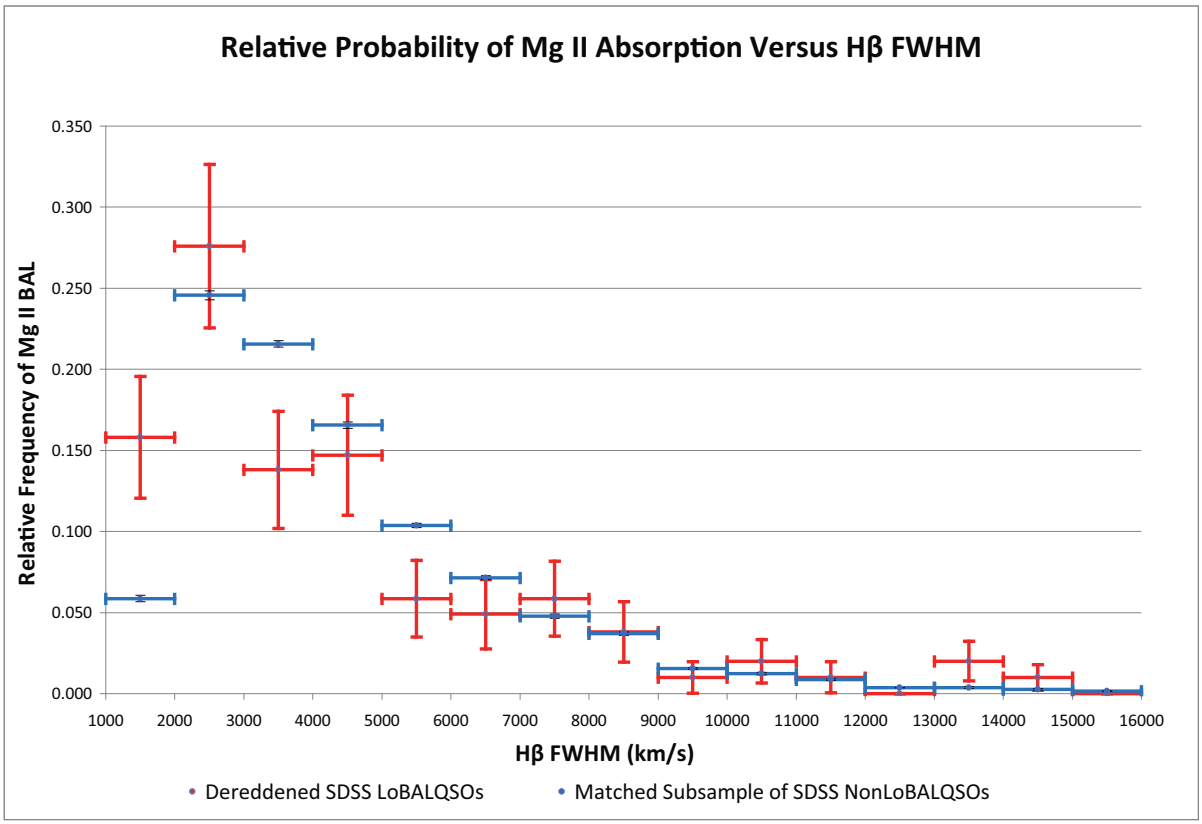

Fig. 3.— The distributions of Hβ FWHM of LoBALQSOs and "matched" sample of non-LoBALQSOs from DR7. The matched sub-sample is created from the full SDSS nonLoBALQSOS sample by the condition $L_{optical} > 9 \times 10^{44}$ ergs/s. Comparison to Figure 1 shows that the excess of narrow line profiles less than 2,500 km/s in the LoBALQSO population persists. The error bars are based on binomial statistics.

samples in the last two rows of Table 1, that are derived from the $L_{optical} > 9 \times 10^{44}$ ergs/s sample with the additional constraint that the O III luminosity is bounded from above by $L_{OIII} < 10^{43}$ ergs/s or $L_{OIII} < 8 \times 10^{42}$ ergs/s. A statistically significant correlation exists - although the strength of the correlation seems somewhat diminished relative to the sample (two rows above in Table 1) without a threshold on L_{OIII}. There is a trend in Table 1, as the L_{OIII} maximum threshold is lowered and the average L_{OIII} decreases in the three samples defined by $L_{optical} > 9 \times 10^{44}$ ergs/s, the difference between the partial distribution of Hβ FWHM and the partial distribution of Hβ FWHM in the LoBALQSO sample becomes less statistically significant. This might be expected on the basis of the correlation between Hβ FWHM and L_{OIII} in quasar spectra (Boroson and Green 1992). However, the relevant conclusion drawn from these three samples in Table 1 is that the excess of narrow Hβ line profiles seen in LoBALQSOs is statistically significant more pronounced than would have been expected solely from the consideration of the correlation of L_{OIII} with Hβ.

In summary, we constructed samples of nonLoBALQSOs from SDSS DR7 that straddled the LoBALQSO SDSS DR7 sample in three physical properties, optical luminosity, central black hole mass and Eddington ratio. According to Table 1, regardless of whether the parameters were above or below those of the LoBALQSOs, there was always a highly statistically significant excess of narrow Hβ line profiles for LoBALQSOs. This was shown explicitly for a sample that was well matched in Eddington ratio. It is concluded that these parameters are not the physical origin of the excess narrow line profiles. This conclusion is not an artifact of reddening, as we verified this for de-redden LoBALQSOs. This further motivates our exploration of line of sight effects to produce the excess narrow lines seen in the DR7 LoBALQSO population.

4. Simulating a Preferred Line of Sight

In this section, we consider the distribution of non-LoBALQSO FWHM and simulate what the distribution would appear to be for different preferred ranges of the line of sight. This analysis will allow us to discuss the different orientation dependent models. Anticipating the use of the simulation to check "goodness of fit" of the binned data with a χ^2 test, we want to minimize the number of free parameters in our model of the data. The purpose of this fit is to allow us to model the majority of the sources below 8,000 km/s which comprise 92% of the entire sample. We consider the 8% of sources with larger FWHM as outliers that do not drive the orientation dependent properties of the other 92%. As such, we seek a simple single parameter fit that captures the skewness, peak and width of the distribution of FWHM below 8, 000 km/sec. A distribution with the desired skewness and exponential

type tail is the Gamma distribution that we parameterize as,

$$f(\mathrm{FWHM}) = N(\mathrm{FWHM})^{-(\alpha-1)}[\mathrm{e}^{-\mathrm{FWHM}/V}] \ , \tag{2}$$

where f(FWHM) is the probability density, N is a normalization constant chosen to make the total probability equal to one and V is a free parameter that is in units of km/s. We eliminate the other free parameter, α, by choosing which fit minimizes the χ^2 residuals. The result is indicated visually in Figure 4, the $\alpha = 5$ plot is a more accurate fit than the $\alpha = 4$ plot for the best fit values of V. This discriminant is driven by the large residuals generated at low FWHM for $\alpha = 4$. Fine tuning the parameters does not change the fit significantly. No simple parametric distribution will fit the data in Figure 4 with high statistical probability in a χ^2 goodness of fit test. However, as stated above, this theoretical one parameter distribution with $\alpha = 5$ and V a function of the distribution of the line of sight is adequate for estimating the gross properties of the skewness, variance and mean of the distribution that are induced by line of sight effects with the exception of the few percent of outliers residing at high FWHM.

We note that the fit for the full sample of nonLoBALQSOs, GAMMA($\alpha = 5$, $V = 775$ km/sec), works equally well for the matched subsample that was described in the last section. Figure 5 shows that the fit to the matched Eddington ratio subsample of nonLoBALQSOs from section 3 is very similar to that of the full sample of nonLoBALQSOs. The figure clearly shows very little difference between the bin populations of the matched and full samples. There is more scatter in the matched sample than for the full sample because there are less than 19% as many sources in the matched Eddington ratio sample.

In order to simulate the change in the distribution of FWHM of DR7 QSOs in Figure 4, if a preferred line of sight is specified, we consider the popular notion that the BEL gas is distributed in an equatorial pancake, orthogonal to the jet axis, with a random velocity, v_r, superimposed on an equatorial velocity, v_p, that is predominantly bulk motion from Keplerian rotation Jarvis and McClure (2006); Wills and Browne (1986),

$$FWHM \simeq 2\sqrt{v_r^2 + v_p^2 \sin^2\theta} \ . \tag{3}$$

In Wills and Browne (1986), it is suggested that $(v_r/v_p)^2 \approx 0.1$. In general there must be a huge range of these ratios in QSOs, but the Wills and Browne (1986) value represents a characteristic average value over the many QSO environments. Thus, we parameterize equation 3 as

$$FWHM \approx \sqrt{0.1 + sin^2\theta}\, v_{blr} \ , \tag{4}$$

where v_{blr} is a characteristic dispersion velocity of the BLR. The analytic forms in equations (2) and (4), allow us to transform the theoretical $\alpha = 5$ distribution in Figure 4, to different

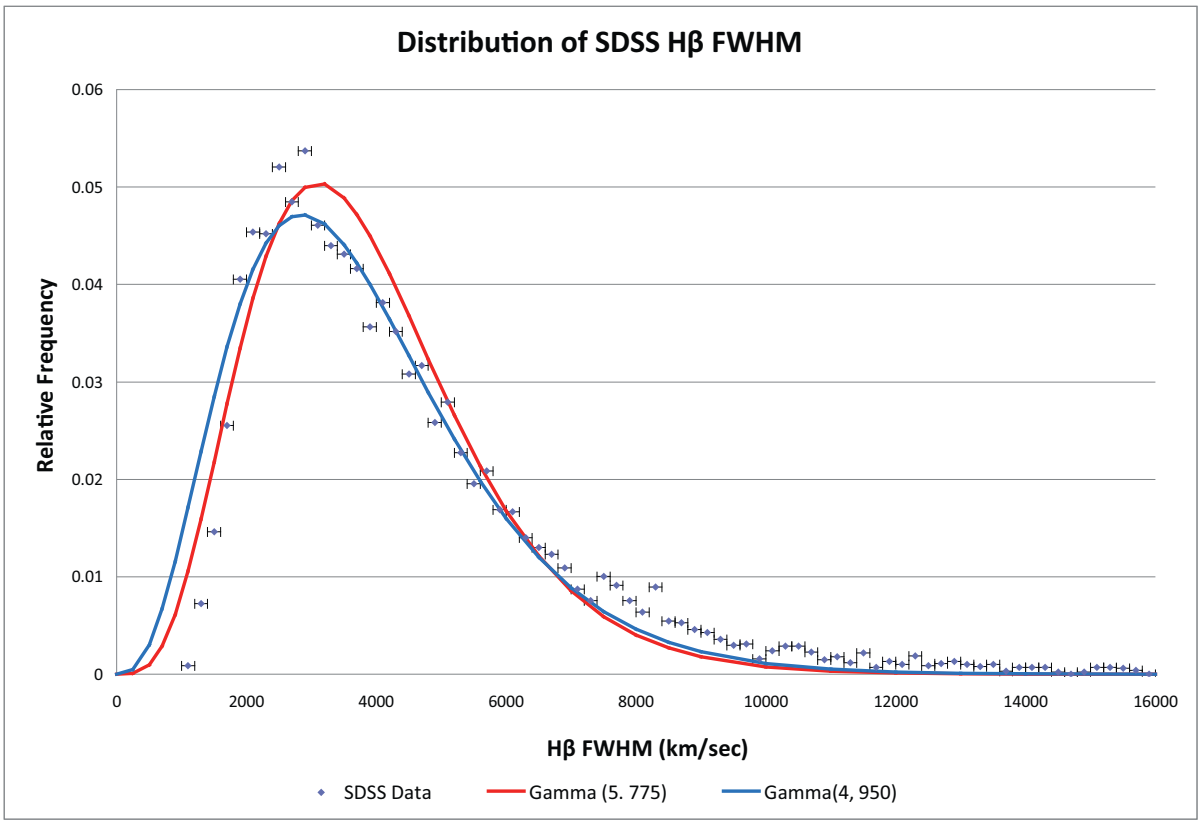

Fig. 4.— Comparison of the theoretical Gamma distributions of Hβ FWHM of non-LoBALQSOs from DR7 for GAMMA(α = 4, V = 950 km/sec) and GAMMA(α = 5, V = 775 km/sec). The distribution, GAMMA(α = 5, V = 775 km/sec), provides a much better fit to the sharply rising low side of the peak of the distribution.

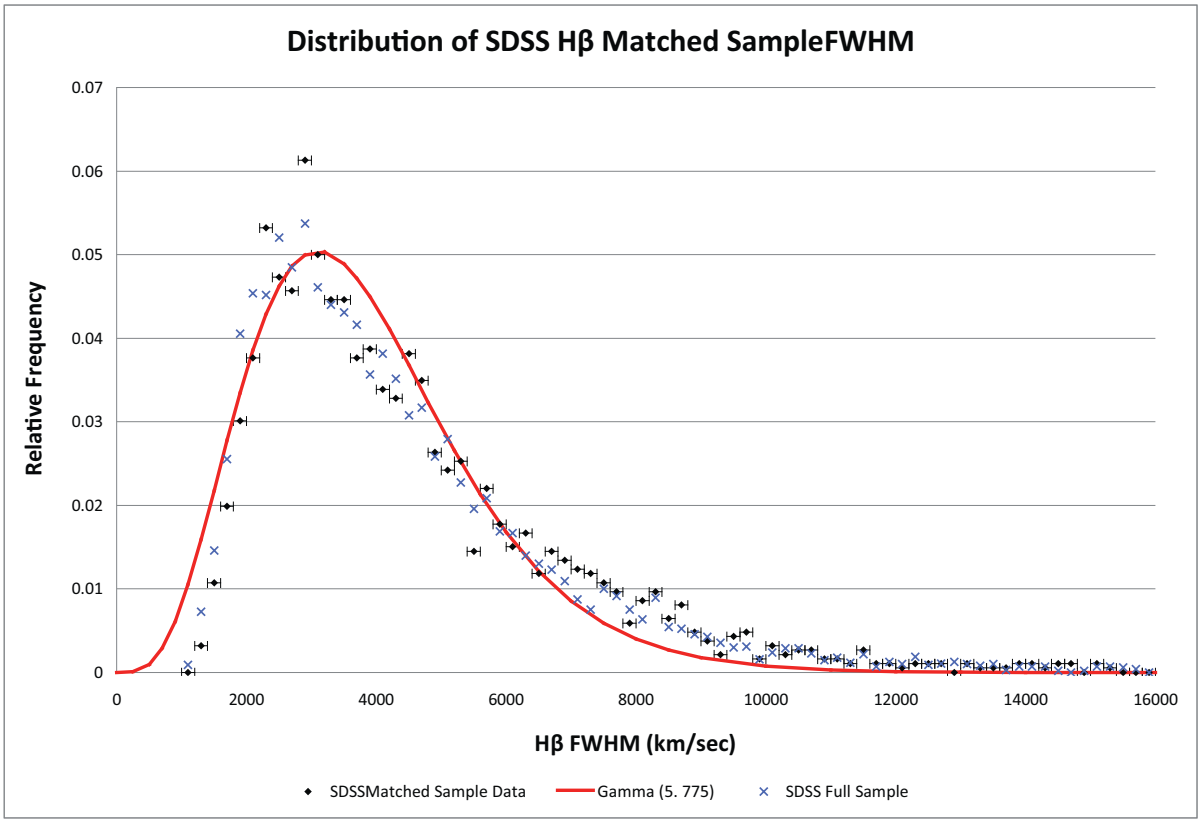

Fig. 5.— Comparison of the theoretical Gamma distribution of Hβ FWHM of non-LoBALQSOs,GAMMA(α = 5, V = 775 km/sec) from Figure 4 and the distribution of Hβ FWHM of the matched subampample of nonLoBALQSOs. The matched sub-sample is created from the full SDSS nonLoBALQSOS sample by the condition $L_{optical} > 9 \times 10^{44}$ ergs/s. We also show the similarity of the distribution of the full sample of DR7 nonLoBALQSOs and the matched sample.

specified ranges of the line of sight. First, we invoke the results of Barthel (1989) that are the basis of the "standard model of QSOs" in Antonucci (1993), QSOs are viewed at a random distribution of lines of sight within a range of about 45° (which represents the half opening angle of the molecular torus) of the jet axis (the normal to the accretion disk). The transformed distribution is determined by a change of coordinates defined by the mapping of the distribution of velocities, v_{blr} to a specified line of sight by means of equation (4). This amounts to a change in the single parameter V in equation (2) (and the induced change in probability normalization, N). The distribution of v_{blr} is defined by the parameter $V = 1314\,\mathrm{km/s} \equiv V_{BLR}$. For a given distribution of line of sights, $g(\theta)$, the distribution parameter V transforms as $V = FV_{BLR}$, where

$$F = \frac{\int g(\theta)\sqrt{0.1 + sin^2\theta}\,\sin\theta d\,\theta}{\int g(\theta)\,\sin\theta d\,\theta}\ . \tag{5}$$

For the uniform distributions (in terms of solid angle) considered below, $g(\theta)$ is just a step function. The results are presented in Figure 6.

In Figure 6, the distributions have the following significance,

- The uniform distribution of line of sight angles, $0° < \theta < 45°$, designated as "Uniform [0, 45]" is the Barthel (1989) empirical distribution for all QSOs
- The uniform distribution of line of sight angles, $0° < \theta < 25°$, designated as "Uniform [0, 25]" is the Punsly (1999b) theoretical distribution for LoBALQSOs
- The uniform distribution of line of sight angles, $80° < \theta < 85°$, designated as "Uniform [80, 85]" is the Murray et al (1995) theoretical distribution for LoBALQSOs
- The uniform distribution of line of sight angles, $40° < \theta < 50°$, designated as "Uniform [40, 50]" is the Elvis (2000) phenomenological distribution for BALQSOs

We discuss these simulated distributions in the context of the DR7 LoBALQSO FWHM distribution in the next section.

5. Analysis of the Simulated Distributions

In Table 2, we attempt to quantify how well the different theoretical models describe the data. The columns from left to right are first the model description, then the next two columns are the degrees of freedom and the χ^2 statistic if the continuous distribution

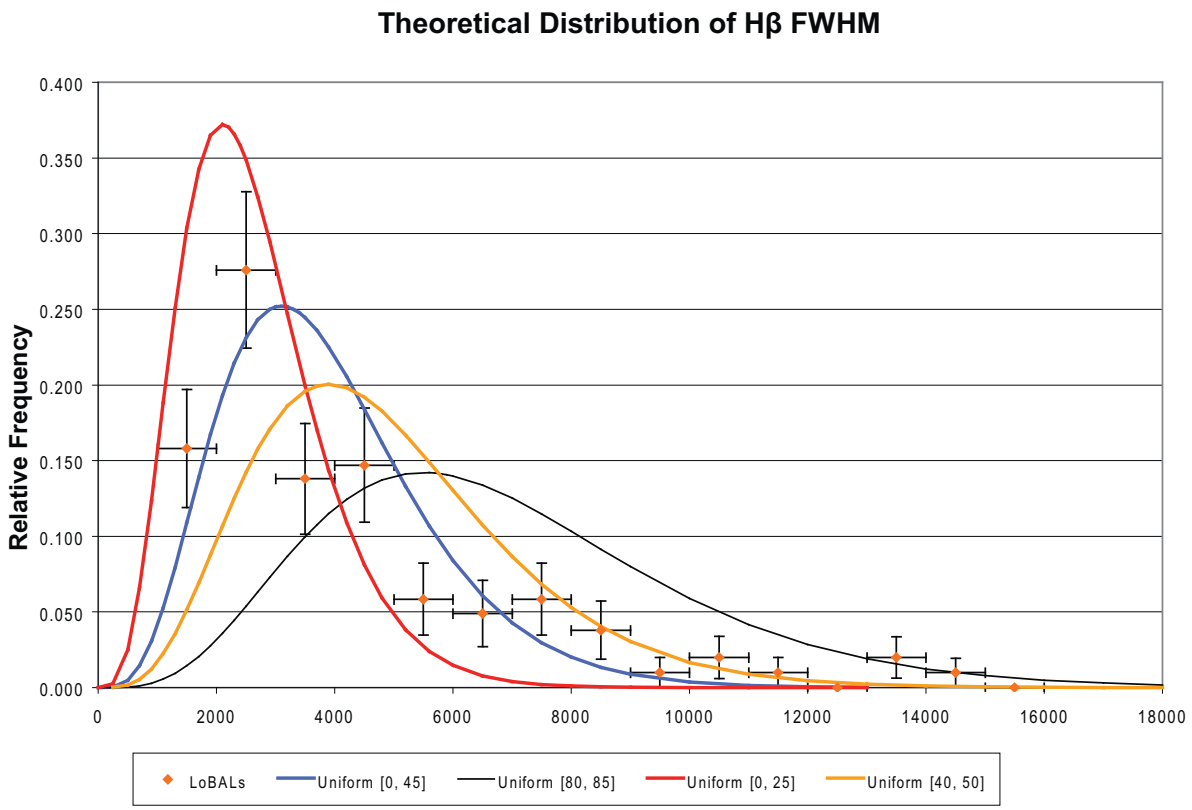

Fig. 6.— Comparison of the simulated distributions of Hβ FWHM for different distributions of the line of sight. Note that none of these represent the DR7 LoBALQSO data very well. As the line of sight becomes more polar the distribution is skewed towards smaller FWHM.

is binned in 1,000 km/s cells as in Figure 1. In order to make a χ^2 analysis plausible, we need a theoretically expected population of at least 5 per bin. Thus, we combine all the LoBALQSOs with a FWHM > 7,000 km/s into one final bin (a total of 7 bins are combined). The fourth column is the probability, P_{χ^2}, that we can reject the hypothesis that the data is described by the theoretical distribution. Note that we have abbreviated the "Uniform" Distribution by the symbol "U" in Table 2. We added the K-S "D" statistic in the fifth column which is a goodness of fit measure that is not sensitive to small bin populations. The K-S probability that we can reject the hypothesis that the data is described by the theoretical distribution is listed in the last column.

The only fits that are not rejected by one or both of the statistical tests are the two component fits in rows 4 through 10 (see Figure 7). Any composite fit that is composed of the range 55% Uniform [0, 25] and 45% Uniform [80, 85] to 75% Uniform [0, 25] and 25% Uniform [80, 85] can not be rejected on a statistical basis. Note that the equatorial model is rejected by this statistical analysis. The distribution, (0.67)(Uniform [0, 25])+ (0.33)(Uniform [80, 85]), represents the peak fairly accurately and it is also fits the high velocity tail reasonably well.

6. Discussion

There have been other discussions involving the possible orientation of the line of sight to the BAL gas which we discuss below. What distinguishes our methods from previous efforts is the very direct determination of the geometry. Previous discussions in the literature involved indirect physical arguments that invariably relied upon unverifiable assumptions. In this section we discuss our results in the context of previous discussions of orientation and line widths.

Table 2: Goodness of Fit to the Line of Sight Models

Model	df	χ^2	P_{χ^2}	D	P_{KS}
U [0, 45]	6	11.85	0.934	0.141	0.97
U [40, 50]	6	45.12	> 0.9999	0.235	> 0.999
U [80, 85]	6	226.79	> 0.9999	0.433	> 0.999
(0.75)(U [0, 25]) + (0.25)(U [80, 85])	4	3.24	0.481	0.118	0.87
(0.70)(U [0, 25]) + (0.30)(U [80, 85])	4	3.06	0.452	0.086	0.71
(0.67)(U [0, 25]) + (0.33)(U [80, 85])	4	3.20	0.473	0.076	0.66
(0.60)(U [0, 25]) + (0.40)(U [80, 85])	4	4.30	0.633	0.064	0.60
(0.55)(U [0, 25]) + (0.45)(U [80, 85])	4	5.81	0.876	0.088	0.73
(0.55)(U [0, 25]) + (0.45)(U [40, 50])	4	4.40	0.645	0.130	0.93

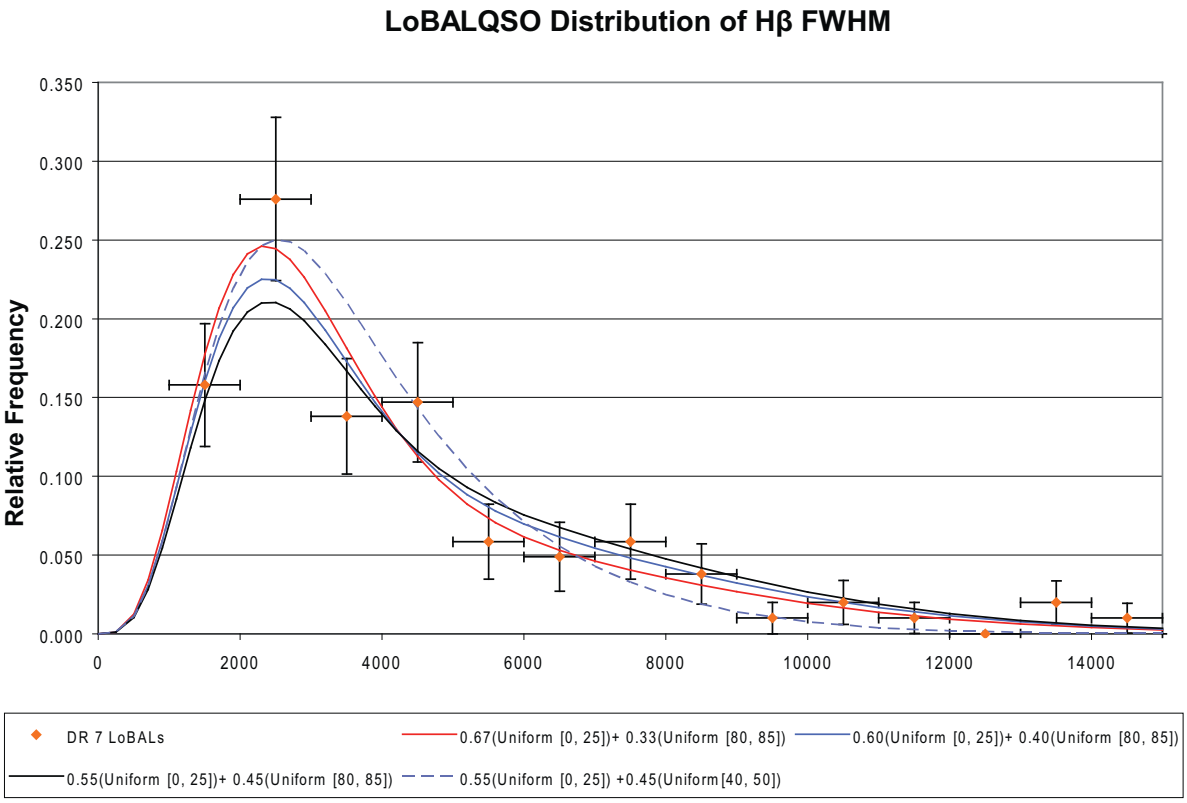

Fig. 7.— Comparison of the simulated two component distributions of Hβ FWHM for lines of sight defined by, (0.67)(Uniform [0, 25]) + (0.33)(Uniform [80, 85]), (0.60)(Uniform [0, 25]) + (0.40)(Uniform [80, 85]), (0.55)(Uniform [0, 25]) + (0.45)(Uniform [80, 85]) and (0.55)(Uniform [0, 25]) + (0.45)(Uniform [40, 50]). The model (0.67)(Uniform [0, 25]) + (0.33)(Uniform [80, 85]) is tantamount to notion that 2/3 of the LoBALQSOs are polar wind sources that were proposed in the theoretical model of Punsly (1999b) and 1/3 of the LoBALQSos are equatorial winds sources proposed in the theoretical wind model of Murray et al (1995).

6.1. Polarization

Historically, the observed elevated polarization of BALQSOs has been used as an argument that ordinary quasars appear as BALQSOs because the line of sight is just above the dusty torus in the standard model (Schmidt and Hines 1997; Ogle 1997; Lamy and Hutsemekers 2004). In axisymmetric geometries, equatorial lines of sight produce higher degrees of polarization than polar lines of sight. Furthermore, the putative "equatorial" line of sight to the BAL gas is consistent with the idea that stray dusty gas above the torus is responsible for the reddening that is observed in the UV continuum (Schmidt and Hines 1997). This argument is indirect and very circumstantial. First of all, the elevated degree of polarization is not that high for most BALQSOs, the median polarization is $\gtrsim 1\%$. Theoretically, this value can be accommodated in any geometry due to modest attenuation of the continuum (see below) by the BAL wind which enhances the prominence of the scattered light (Punsly 1999b). Secondly, two of the most polarized BALQSOs, FIRST 1556+3517, Brotherton et al (1997), and MRK 231, Smith et al (1995), have polarizations $\approx 13\%$ in the near UV and are now know to be polar objects (Ghosh and Punsly 2007; Reynolds et al 2009). Furthermore, both of these polar sources are heavily reddened (Najita et al 2000; Smith et al 1995). Thus, these two well studied examples show that one can not use the enhanced polarization of BALQSOs and reddening of the continuum as an argument for equatorial BAL winds.

Theoretically, it was pointed out in Punsly (1999b) that the rare outlier polarizations of $> 3\%$ can be obtained in a polar line of sight if the assumption of axisymmetry is dropped. Modest reddening is a natural consequence of the polar wind model. There is significant attenuation from scattering in the theoretical models as the continuum radiation field propagates through the polar BAL wind (Punsly 1999b). The amount of attenuation is consistent with the statistically based estimates of Goodrich (1997), $\sim 30\%$ to 50%. The UV must shine through larger optical depths (the inner regions of the wind) than the optical (outer regions of the polar wind), hence the polar models naturally produce reddening. Excessive reddening requires entrainment of dusty material on larger scales.

The equatorial line of sight argument is very dependent on the assumption of axisymmetry for the scattering surface, which is apparently not justified (as noted above, the extreme outlier elevated polarizations can occur in polar geometries once the perfect axisymmetry assumption is dropped and evidenced by the high polarization in the polar sources MRK 231 and FIRST 1556+3517). Within these equatorial models the LoBALQSOs are viewed even closer to the equator than other BALQSOs (Murray et al 1995). However, the fits in Table 2 and Figure 6 indicates that this model cannot explain the DR7 data. The equatorial view enhances large FWHM and cannot explain the excess of small FWHM seen in the DR7 LoBALQSO data. Figure 7 indicates that at most $\approx 1/3$ of the LoBALQSOs are equato-

rial outflows. The method used in this paper to determine the line of sight requires less physical interpretation of the data and less assumptions than the polarization and reddening argument.

6.2. Radio Luminosity and Orientation

The anti-correlation between radio luminosity and the degree of absorption in LoBALQSOs was used in Dai et al (2010) as an argument that most LoBALQSOs must be viewed through an equatorial BAL wind. They proposed that the LoBALQSOs tend to be weak radio sources because the radio emission is vastly weaker for perpendicular lines of sight to a relativistic jet. They made an analogy to powerful radio loud sources in which radio cores are enhanced by Doppler beaming (Wills and Browne 1986). It is far from obvious that there is a strong connection between radio loud quasar jets and the weak radio emission seen in most LoBALQSOs. The authors assume without justification that every LoBALQSO jet is identical (bulk Lorentz factor, power, etc.) and the difference in single point radio flux density is due to the line of sight. Core flux is not a good orientation indicator, since the same type of logical argument presented in Dai et al (2010) leads to the erroneous conclusion that radio quiet quasars must be viewed near the equator because they are radio weak (compared to radio loud sources). The true orientation indicator is the ratio of core to lobe flux density as noted in Wills and Browne (1986). The data analysis presented in our paper suggests the alternative explanation that the mechanism that launches the BAL wind tends to inhibit the central engine that drives the powerful radio jet or the ability of that jet to propagate.

6.3. Two Component Models

The only other attempt that we know of to arrive at the distribution of lines of sights to BALQSOs was in Borguet and Hutsemekers (2010). They fit CIV absorption (HiBALQSOs) line profiles in a parametric model. Unfortunately, the model is completely adhoc, it is comprised of a spherical fast wind with with a slower narrow equatorial wedge inserted. The bulk of the solid angle is called a polar wind, yet it is nearly spherical. Every parameter is adhoc, from the launch point, to the distribution of the broad emission line gas, the density and the velocity. They found the need for both components, in general, to reproduce the line shapes. In Proga and Kallman (2004), the numerical simulations showed that by adjusting the parameters one could get polar winds, equatorial winds, mid-latitude winds as in Elvis (2000) or virtually any combination thereof. However, given the adhoc nature of the models

in Borguet and Hutsemekers (2010), it is very unclear if there is any physical significance to the parametric variations that led these authors to conclude that most sources are viewed along the equatorial plane. The driving piece of logic was that deep zero velocity absorption (P Cygni type) lines mean that one is viewing the BAL wind along the eqautor. However, FIRST1556+3517 has deep zero velocity absorption in MgII, Brotherton et al (1997), and it is polar.

7. Conclusion

In this paper, we used the distribution of Hβ FWHM in the SDSS DR7 data release to estimate the distribution of lines of sight to LoBALQSOs. Our analysis indicates that predominantly equatorial outflow is ruled out for LoBALQSOs. We also find that the data is not well represented by random lines of sight. The distribution has an excess of sources with narrow Hβ that is best fit by assuming two classes of LoBALQSOs, the majority ($\approx 2/3$) are polar outflows and the remainder are equatorial outflows. By choosing a variety of subsamples of nonLoBALQSOs matched in redshift that straddle the values of luminosity, black hole mass and Eddington ratio of the de-reddened LoBALQSO sample, we find that the narrow line excess in the LoBALQSO sample persists in all cases and therefore eliminate the possibility that the excess narrow lines seen in LoBALQSOs arise from the physical properties of the central black hole accretion system such as Eddington ratio.

We make one more comment on the important work of Ganguly et al (2007). They measured the FWHM of the Mg II of HiBALQSOs and non-BALQSOs. There was no statistical difference. This implies random lines of sight to HiBALQSOs per the methods discussed here. However, they chose to combine mini-BALQSOs and BALQSOs to increase sample size. These types of sources are not BALQSOs in the conventional sense and the results might not be reliable. The DR5 statistical analysis of Zhang et al (2010) indicate that these types of sources (mini-BALQSOs have a large overlap in definition with the intermediate width absorption line sources of Zhang et al (2010)) tend to resemble non-BALQSOs more than BALQSOs in many spectral properties. Furthermore, one must use caution in the interpretation of Mg II FWHM with HiBALQSOs, since there might be low level absorption in the continuum blueward of Mg II that might skew continuum estimates. It would be hard to segregate this effect and quantify its impact on the sample. This type of analysis is best done without resorting to resonance lines for FWHM estimates. Thus, Hβ is preferred over Mg II.

Based on these considerations mentioned above, it would be important to reproduce the analysis for LoBALQSOS presented here with a similar study for Hi BALQSOs. One could

select high redshift HiBALQSOs from SDSS and observe the Hβ profiles in the IR.

We would like to thank Robert Antonucci for sharing his expertise and insights. We were also fortunate to benefit from many interesting comments from Paola Marziani. We would also like to thank an anonymous referee who offered many ideas that improved the manuscript.

REFERENCES

Antonucci, R.J. 1993, Annu. Rev. Astron. Astrophys. **31** 473

Antonucci, R.J., Kinney, A., Ford, H. 1989, ApJ **342** 64

Barthel, P. 1989, ApJ **336** 606

Becker, R.H., Gregg, M.D., Hook, I.M., McMahon, R.G., White, R.L., & Helfand, D.J. 1997, ApJL textbf479 93

Becker. et al 2000, ApJ **538** 72

H.Borguet, B. and Hutsemekers, D. 2010 to appear in A & A, arXiv:1003.2386

Brotherton, M., Tran, H., Van Bruegel, W., Dey, A. and Antonucci, R. 1997 ApJL **487** 113

Brotherton, M., De Breuck, C., Schaefer, J. 2006 MNRAS **372** 58

Boroson, T. 2002, ApJ **565** 78

Boroson, T. and Green, R. 1992, ApJS **80** 109

Corbin, M. and Francis, P. 1994, AJ **108** 2016

Corbin, M. and Borosn, T. 1996, ApJS **107** 69

Dai, X., Shankar, F., Sivakoff, G. 2010 submitted to MNRAS http://adsabs.harvard.edu/abs/2010arXiv1004.0700D

Elvis, M. 2000 ApJ **545** 63

Gallagher, S. et al 2007 ApJ **665** 157

Ganguly, R. et al 2007 ApJ **665** 990

Gibson, R. et al 2009 ApJ **692** 758

Ghosh, K. and Punsly, B. 2007 ApJL **661** 139

Goodrich, R. 1997 ApJ **474** 606

Hewett, P. and Foltz, C., 2003 AJ **125** 1784

Jarvis, M., McClure, R. 2006, **369**, 182

Kaspi, S. et al 2000, ApJ **533** 631

Kellermann, K. I., & Pauliny-Toth, I. I. K. 1969 ApJ, **155**, L71

Lamy, H. and Hutsemekers, D. 2004 A & A, **427**, 107

Lind, K., Blandford, R. 1985, ApJ **295** 358 345

Maiolino, R.. et al 2002, A & A **375** 25

Marscher, A. et al 1979, ApJ **233** 498

McClure, R., Jarvis, M. 2002, MNRAS **337** 109

Montenegro-Montes, F. et al 2008, MNRAS **388** 1853

Murray, N. et al 1995, ApJ **451** 498

Najita, J., Dey, A., Brotherton, M. 2000 AJ **120** 2859

Ogle, P. 1997 in ASP Conf. Ser. 128, **Mass Ejection from Active Nuclei** ed, N.Arav, I. Shlosman and R.J. Weymann (San Francisco: ASP) 78

Proga, Kallman, T. ApJ 2004 **616** 688

Punsly, B. 1999, ApJ **527** 609

Punsly, B. 1999, ApJ **527** 624

Reichard, T.A., et al. 2003, AJ **126** 2594

Reynolds, C., Punsly, B. Kharb, P., O'Dea, C. and Wrobel, J. 2009, **706** 851

Schmidt, G., and Hines, D. 1997 in ASP Conf. Ser. 128, **Mass Ejection from Active Nuclei** ed, N.Arav, I. Shlosman and R.J. Weymann (San Francisco: ASP) 106

Smith, P. et al 1995, ApJ **444** 146

Sulentic, J. et al 2006, MxAA **42** 23

Trump, J. et al 2006, ApJS **165** 1

Vestergaard, M. and Peterson, B. 2006, ApJ **641** 689

Weymann, R.J., Morris, S.L., Foltz, C.B., Hewett, P.C. 1991, ApJ **373**, 23

Weymann, R. 1997 in ASP Conf. Ser. 128, **Mass Ejection from Active Nuclei** ed, N.Arav, I. Shlosman and R.J. Weymann (San Francisco: ASP) 3

Willott, C., Rawlings, S., Grimes J. 2003, ApJ **598**, 909

Wills, B., Brotherton, M 1995, ApJL **448** 81

Wills, B.J., Browne, I.W.A. 1986 ApJ **302** 56

Zhang, S. et al 2010 ApJ **714** 367

Zhou, H. et al 2006 ApJ **639** 716